

Review

Advances in All-Solid-State Passively Q-Switched Lasers Based on Cr⁴⁺:YAG Saturable Absorber

Jingling Tang ^{1,2}, Zhenxu Bai ^{1,2,3,*}, Duo Zhang ^{1,2}, Yaoyao Qi ^{1,2}, Jie Ding ^{1,2}, Yulei Wang ^{1,2} and Zhiwei Lu ^{1,2}

¹ Center for Advanced Laser Technology, Hebei University of Technology, Tianjin 300401, China; tangjinglingjiguang@outlook.com (J.T.); zd1223860027@163.com (D.Z.); qiyao@hebut.edu.cn (Y.Q.); dingjie@hebut.edu.cn (J.D.); wyl@hebut.edu.cn (Y.W.); zhiweilv@hebut.edu.cn (Z.L.)

² Hebei Key Laboratory of Advanced Laser Technology and Equipment, Tianjin 300401, China

³ MQ Photonics Research Centre, Department of Physics and Astronomy, Macquarie University, Sydney, NSW 2109, Australia

* Correspondence: zxbai@hebut.edu.cn

Abstract: All-solid-state passively Q-switched lasers have advantages that include simple structure, high peak power, and short sub-nanosecond pulse width. Potentially, these lasers can be applied in multiple settings, such as in miniature light sources, laser medical treatment, remote sensing, and precision processing. Cr⁴⁺:YAG crystal is an ideal Q-switch material for all-solid-state passively Q-switched lasers owing to its high thermal conductivity, low saturation light intensity, and high damage threshold. This study summarizes the research progress on all-solid-state passively Q-switched lasers that use Cr⁴⁺:YAG crystal as a saturable absorber and discusses further prospects for the development and application of such lasers.

Keywords: laser; Cr⁴⁺:YAG; all-solid-state; passively Q-switch



Citation: Tang, J.; Bai, Z.; Zhang, D.; Qi, Y.; Ding, J.; Wang, Y.; Lu, Z. Advances in All-Solid-State Passively Q-Switched Lasers Based on Cr⁴⁺:YAG Saturable Absorber. *Photonics* **2021**, *8*, 93. <https://doi.org/10.3390/photonics8040093>

Received: 9 February 2021

Accepted: 22 March 2021

Published: 27 March 2021

Publisher's Note: MDPI stays neutral with regard to jurisdictional claims in published maps and institutional affiliations.



Copyright: © 2021 by the authors. Licensee MDPI, Basel, Switzerland. This article is an open access article distributed under the terms and conditions of the Creative Commons Attribution (CC BY) license (<https://creativecommons.org/licenses/by/4.0/>).

1. Introduction

All-solid-state passively Q-switched lasers have the characteristics of simple structure, small size, and broad application potential in areas, such as high-precision processing, laser medical treatment, and laser communication. As these lasers do not require complex extra-cavity modulation devices or high stability of their light source in addition to also possessing high system reliability, they can be applied to various complex environments, including high precision ranging, space detection, and radar [1–3]. Materials commonly used for passive Q-switches are organic dyes, doped crystals, and semiconductors.

A Cr⁴⁺:YAG crystal has a wide absorption band and saturable absorption characteristics at 0.9–1.2 μm. When compared with other saturable absorbers, Cr⁴⁺:YAG crystal has the advantages of large ground-state absorption cross-section (~10⁻¹⁸ cm²), high doping concentration (~10¹⁸ cm⁻³), good thermal conductivity, low saturated light intensity, high damage threshold (500 MW/cm²), stable physical properties, and long service life. Therefore, it is an ideal Q-switch material for Nd³⁺-doped and Yb³⁺-doped solid-state lasers [4]. Cr⁴⁺:YAG has three main absorption bands: 0.48, 0.63, and 1.06 μm. The 0.48 and 0.63 μm absorption bands are in the visible light region, and the absorption coefficients of the two absorption bands are relatively large, but the absorption of Cr⁴⁺:YAG crystal in these two bands is due to the transfer of Cr⁴⁺ charge in the crystal and the color center, rather than the saturable absorption characteristics of the Cr⁴⁺:YAG crystals. The absorption of Cr⁴⁺:YAG crystals in the 1.06 μm absorption band is caused by the energy level transition of the particles in Cr⁴⁺:YAG, so the 1.06 μm absorption band is an important basis for reflecting the saturable absorption characteristics of Cr⁴⁺:YAG crystals. The absorption spectrum of Cr⁴⁺:YAG is shown in Figure 1.

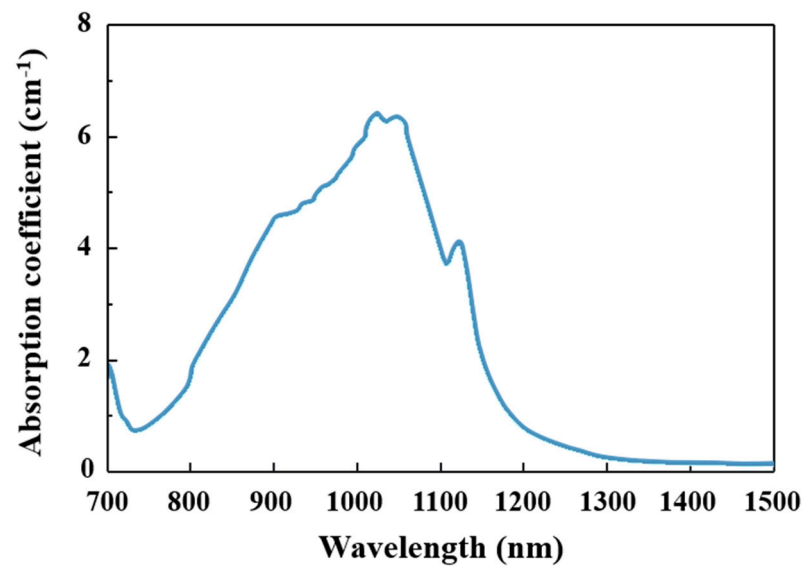


Figure 1. Absorption spectrum of Cr⁴⁺:YAG.

Since the 1990s, the emergence of various saturable absorber doped with Cr⁴⁺ ion has attracted attention, and a series of important advances have been made. Figure 2 illustrates the timeline of advances in all-solid-state passively Q-switched lasers based on Cr⁴⁺-doped crystals.

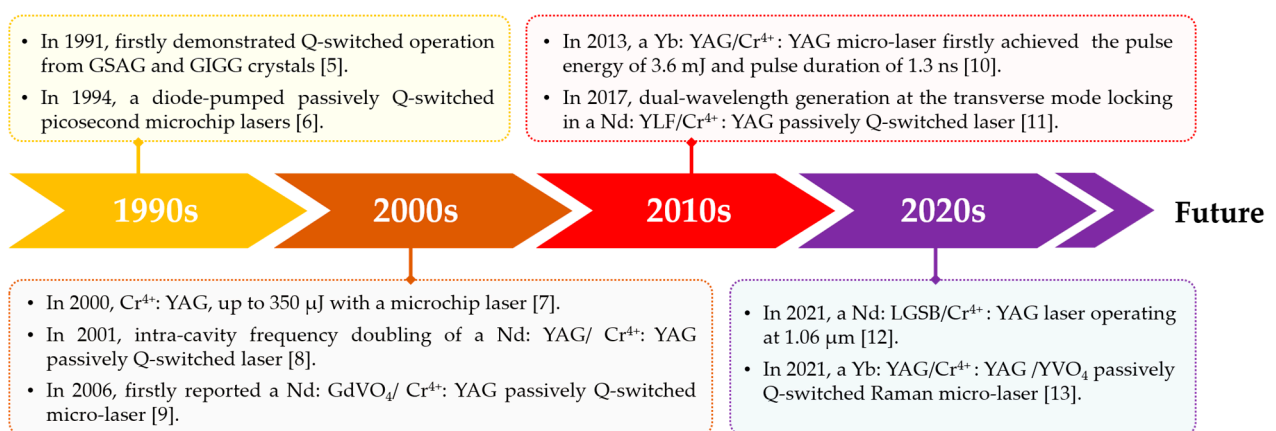


Figure 2. Timeline of advances in all-solid-state passively Q-switched lasers based on Cr⁴⁺-doped crystals [5–13].

This study summarizes the research progress on all-solid-state passively Q-switched lasers that use Cr⁴⁺:YAG crystal as the saturable absorber, including Nd³⁺-doped passively Q-switched laser, Yb³⁺-doped passively Q-switched laser, and other ion-doped lasers. Potential future developments and applications are also discussed.

2. Research Progress

2.1. Nd³⁺-Doped Passively Q-Switched Lasers

In recent years, LD-pumped Nd³⁺-doped lasers have been widely developed and have potential applications in scientific research, infrared remote sensing, etc. The energy level structure of an Nd³⁺ ion in Nd:YAG is illustrated in Figure 3 [4]. The 1.06 μm transition provides the lowest threshold laser lines in Nd:YAG. The main laser transition occurs at 1064 nm due to the ⁴F_{3/2}→⁴I_{11/2} transition, and the main pump band is shown in Figure 3.

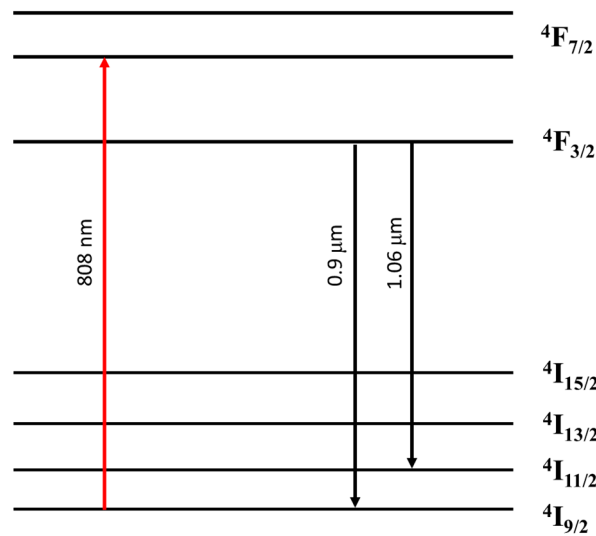


Figure 3. Energy level structure of Nd^{3+} in Nd:YAG.

According to this diagram, the emission wavelengths of the Nd^{3+} ions coincide with the absorption wavelengths of the Cr^{4+} :YAG crystal, specifically in the commonly used 1.06 μm band. Therefore, using Nd^{3+} -doped passively Q-switched lasers with Cr^{4+} :YAG crystal as the saturable absorber has garnered scientific interest.

2.1.1. Research Progress on Passively Q-Switched Lasers in the Infrared Band

In 2016, Tasi et al. first reported spatiotemporal chaos under a stationary spatial distribution of polarization. A period-doubling route to chaos was observed in a passively Q-switched Nd:GdVO₄ laser beam with azimuthal polarization [14]. Figure 4 demonstrates the testing setup and output results.

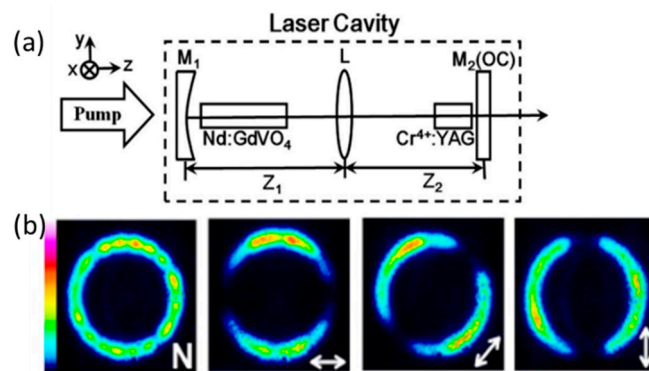


Figure 4. Nd:GdVO₄/Cr⁴⁺:YAG passively Q-switched vortex laser. (a) Experimental setup. (b) Angular polarization output.

Due to stringent emission norms, increasing demands for higher efficiency and reliable engine operation, and rapid depletion of petroleum resources, extensive research work is being conducted to explore advanced combustion and ignition technologies as well as the use of alternative fuels for internal combustion engines [15,16]. Laser ignition allows precise control of ignition energy deposited in ignition plasma and therefore increases the efficiency of the engine, which has led to increased research on laser ignition in the last few years [17–22].

With the development of crystal growth technology, studies have found that controllable Hermite–Gauss (HG), Ins–Gauss (IG), and Laguerre–Gauss (LG) mode lasers can be obtained from different orientations of Nd:YVO₄ crystals [23,24]. Dong et al. have pumped

Nd:YVO₄ crystals in a tilted, unfocused manner and realized HG_{3,0}, HG_{3,3}, HG_{3,6}, HG_{6,6}, HG_{12,3}, and HG_{6,13} mode laser outputs [25]. In 2019, Zhang et al. studied the effects of Cr⁴⁺ ions on the formation of IG laser modes in a tilted pumped Nd:YAG/Cr⁴⁺:YAG passively Q-switched laser [26].

YAG and YVO₄ crystals are the most commonly used materials for Nd³⁺ ion doping. However, the output wavelength range of the Nd:YAG, Nd:YVO₄ passively Q-switched laser is limited and cannot produce the specific wavelengths required in various fields. As crystal growth technology has developed, studies have investigated new substrates for Nd³⁺ ion doping, aiming to improve the laser's performance [27–33]. In addition, studies have shown that doping by multiple ions in the same substrate can increase the energy level life of the laser crystal, the crystal's heat dissipation capacity, and enhance its absorption bandwidth as well as increasing the utilization rate of the pump laser [34–37].

To further improve the overall performance of the all-solid-state passively Q-switched laser and solve the problems of thermal effects and timing jitter, studies have covered improvements in pump source [38,39], crystal position [40,41], cavity structure [22,42], Q-switching method [43], and temperature control [44–49]. In 2016, Zheng et al. proposed fast-pulse pumping technology to solve the thermal effect and timing jitter issues [50]; Chen et al. proposed a set of analytical expressions (1) to analyze the time difference between adjacent longitudinal modes of passively Q-switched lasers. An Nd:YAG/Cr⁴⁺:YAG laser was used for experimental verification, and a single longitudinal mode output was realized [51].

$$\Delta t_s = \left[\exp\left(\frac{t_{pump}}{\tau_f}\right) - 1 \right] \frac{\sigma_m - \sigma_n}{\sigma_n} \quad (1)$$

Δt_s : the time difference between the establishment of the *n*th and *m*th longitudinal modes; t_{pump} : pump pulse duration; τ_f : fluorescence lifetime of crystal Nd:YAG; σ_k : the stimulated emission cross-section of the *k*th longitudinal mode, $k = 1, 2, \dots, n, \dots$.

In 2017, Croitoru et al. investigated air breakdown in a static chamber using a passively Q-switched Nd:YAG/Cr⁴⁺:YAG laser. The energy transfer characteristics from a laser pulse to plasma were estimated by investigating the total input energy and local transfer energy [52]. In 2019, Villafana et al. used a periodic simulation model to analyze Nd:YVO₄/Cr⁴⁺:YAG passively Q-switched lasers. This model is suitable for controlling the laser stability in different harmonic ranges [53]. Bai et al. reported a passively Q-switched Nd:YAG/Cr⁴⁺:YAG laser that operates stably at temperatures between −74 and (approximately) 50 °C, or over 100 °C. The experiment used a semiconductor laser diode array for side pumping, which enabled stable laser operation despite large temperature fluctuations [54].

Although all-solid-state passively Q-switched lasers have been utilized in differing fields (scientific research, military, etc.), many applications place strict requirements on the laser's wavelength and overall volume. For example, the field of nonlinear frequency conversion requires single longitudinal mode pulsed laser, and in a vehicle-mounted laser ignition device, the volume of the laser cannot exceed that of the spark plug. To improve the portability of the laser, the gain medium and saturable absorber can be thermally bonded and then used to directly coat both ends of the composite crystal. These design improvements reduce the volume of the laser while ensuring stable laser output [55–57]. Further studies have led to the development of a single longitudinal mode Q-switched laser with increased stability and improved repression of the spatial hole burning effect. These improvements were realized by increasing the pump power, changing the crystal's temperature, adding a modulator, and adopting a ring cavity [49,58–62].

The relaxation time of the first excited state of Cr⁴⁺:YAG is ~3.4 μs, which is much longer than the pulse oscillation time for most cases. Therefore, with low intracavity intensity, most of the population in Cr⁴⁺:YAG crystal is in the ground state, and the transition to higher-lying levels is rather weak. In this condition, Cr⁴⁺:YAG crystal acts as an effective saturable absorber only for Q-switching operation. While the intracavity laser intensity is large enough to reach the saturable absorption of the excited state, the relaxation

time from high energy level to the first excited state is in the sub-nanosecond range. Q-switched mode-locking can then be generated with a single mode-locked pulse duration near the maximum of the Q-switched envelope in the order of picoseconds [63–68].

The gain medium of the all-solid passively Q-switched laser is usually round rod or block, but there are serious thermal lens effects and birefringence effects under high-power pumping, which make the gain medium produce strong optical distortion and limit the output power of the laser. The waveguide laser improves the power by providing one-dimensional control of the thermal lens effect and increasing the width and length of the waveguide doped region. Therefore, combining the waveguide structure with a passive Q-switched crystal can obtain higher peak power pulsed laser output [69–71].

2.1.2. Passively Q-Switched Green Lasers

Green pulsed lasers (490–580 nm) have aroused significant interest because of their potential application to many fields. Three established methods exist for all-solid-state passively Q-switched lasers to achieve visible laser output. One method uses blue-pumped Pr^{3+} , Sm^{3+} , Tb^{3+} , Dy^{3+} , Ho^{3+} , and Er^{3+} passively Q-switched lasers. The second method involves generating a $\sim 1 \mu\text{m}$ pulsed laser, which irradiates a frequency-doubling crystal, and a green laser is emitted [72]. Although this method can generate high peak power, the frequency conversion step from the near-infrared to the green spectral range requires highly stable fundamental frequency laser. This condition leads to overly complex systems. The third method is self-frequency-doubled Nd^{3+} -doped or Yb^{3+} -doped lasers. In this method, a high peak power pulsed laser is obtained by inserting a saturable absorber in the self-frequency-doubled lasers. When compared with the first two methods, the self-frequency-doubled lasers are more compact and effective [73,74].

2.1.3. Passively Q-Switched Raman Lasers

Compact solid-state lasers that can simultaneously emit multiple wavelengths have a wide range of applications, including optical communications, environmental monitoring, and medical instruments. Stimulated Raman scattering enables traditional lasers to achieve stable, concurrent multi-wavelength output. Combining stimulated Raman scattering and LD-pumped passively Q-switched lasers can produce dual-wavelength Raman laser [75–77].

All-solid-state passively Q-switched Raman lasers are the most compact and effective Raman lasers, because the laser medium and the Raman medium are the same crystal. The passive Q-switched Raman lasers have high peak power and narrow pulse width, effectively realizing multi-wavelength output. Owing to its excellent Raman gain, Nd:YVO_4 crystal is often used as a self-Raman medium. In 2016, Lin et al. reported a multi-wavelength passively Q-switched self-Raman laser. Using *c*-cut Nd:YVO_4 as the laser and Raman medium, and $\text{Cr}^{4+}:\text{YAG}$ crystal as the saturable absorber, the self-Raman laser wavelength outputs were 1067.4, 1097.9, 1130.1, and 1163.6 nm [78]. This team achieved 1066.7 and 1168.6 nm Raman laser output using equipment based on Lin et al.'s study [79]. In 2019, Chen et al. reported a *c*-cut $\text{Nd:YVO}_4/\text{Cr}^{4+}:\text{YAG}$ passively Q-switched self-Raman laser, with a maximum average output power of 2.5 W; the highest reported value for a passively Q-switched Raman laser [80]. In 2020, Li et al. reported a multi-wavelength passively Q-switched intracavity Raman laser. In the study, *c*-cut Nd:GdVO_4 and *c*-cut Nd:YVO_4 crystals were used as the self-Raman and Raman medium, respectively. The laser generated simultaneous wavelengths of 1096, 1176, and 1177 nm, with average output power of 47.6, 27, and 44.2 mW, respectively [81].

2.1.4. Passively Q-Switched Vortex Lasers

Helical beams with spiral phase and orbital angular momentum are widely used in particle manipulation, material processing, quantum information, optical imaging, and optical communication. By adding passive Q-switching technology to the vortex laser, more effective vortex beam power scaling can be achieved.

In 2017, Chen et al. analyzed the optimal cavity length required to achieve passive Q-switching in an off-axis pumped Nd:YVO₄/Cr⁴⁺:YAG laser. Additionally, using an external cylindrical mode converter, high-order eigenmodes and geometric modes generated vortex beams with large orbital angular momentum [82]. The experimental and theoretical results are shown in Figure 5.

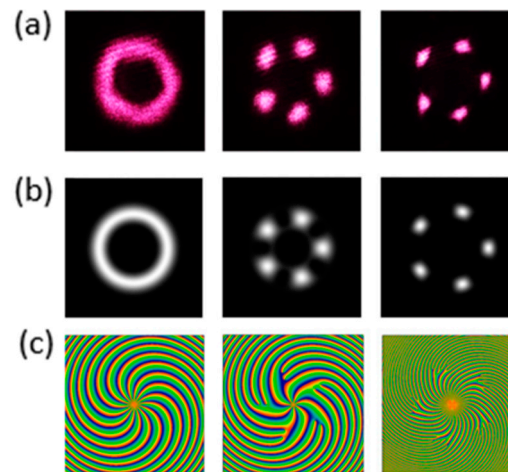


Figure 5. Passive Q-switching in an off-axis pumped Nd:YVO₄/Cr⁴⁺:YAG laser (pump power 3.8 W, off-axis distance 0.55 mm). (a) Experimental results; (b) theoretically calculated results; and (c) theoretically calculated vortex optical phase structure.

In 2018, Tuan et al. studied the output performance of off-axis pumped Nd:YAG/Cr⁴⁺:YAG lasers under different degenerate cavities and obtained a stable output for passively Q-switched laser. Various high-energy vortex beams, with large angular momentum and diverse phase structures, were successfully realized using an astigmatic mode converter (AMC) [83]. In 2019, Pan et al. reported a dual-vortex passively Q-switched microchip laser with controllable orientation and separation. The Nd:YAG/Cr⁴⁺:YAG composite crystal was pumped by an off-center ring beam to achieve a dual-vortex laser pulse with a peak power of 5 kW and pulse width of 3.6 ns. By adjusting the position of the collimating lens, the direction and distance between the two holes in the dual-vortex laser pulse can be varied. The experimental setup, experimental results, and theoretical analysis are shown in Figure 6 [84].

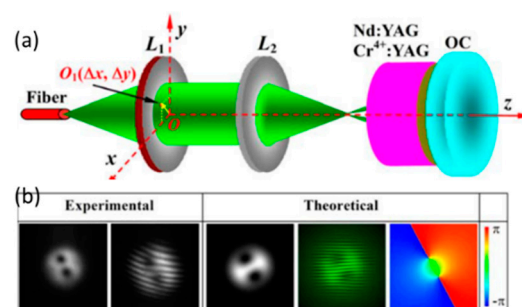


Figure 6. Dual-vortex passive Q-switched microchip laser. (a) Experimental setup and (b) experimental and theoretical model results.

2.2. Yb³⁺-Doped Passively Q-Switched Lasers

When compared with Nd³⁺-doped lasers, Yb³⁺-doped lasers have the advantages of absorption bandwidth, long fluorescence lifetime, large emission cross-section, and low quantum defects. In addition, the Yb³⁺-doped crystal's simple electronic structure, combined with low quantum defects, significantly reduces the thermal load in the ma-

terial [85]. At low temperatures, Yb^{3+} -doped crystals can be used as a four-level laser medium with excellent thermo-optical properties [86]. Figure 7 demonstrates the Yb^{3+} energy level structure of Yb:YAG. The laser has a quasi-three-level operating mechanism because its upper energy level cannot have excited state absorption and up-conversion; particularly, the laser only has a $^2\text{F}_{7/2}$ ground state and $^2\text{F}_{5/2}$ stimulated multiple states with a spacing of $10,000\text{ cm}^{-1}$ [87].

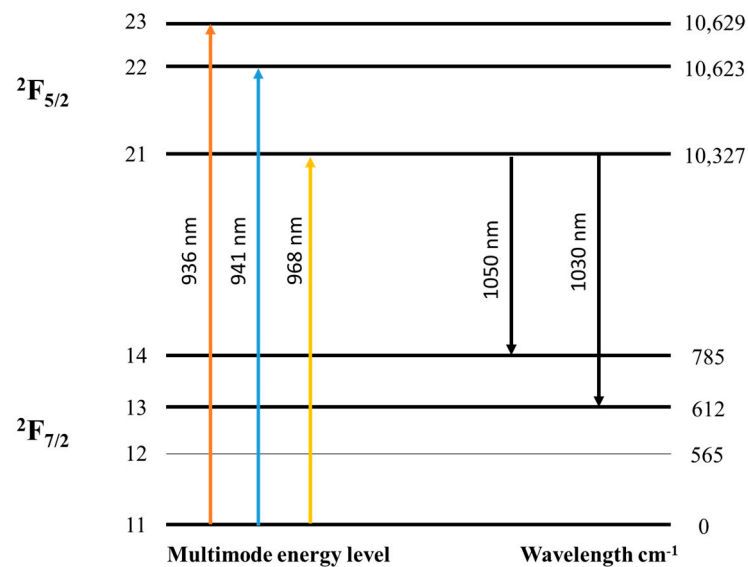


Figure 7. Yb^{3+} energy level structure in Yb:YAG.

In 2017, Šulc et al. studied the influence of temperature on passively Q-switched lasers. Studies have shown that the highest pulse repetition rate of the output light was 38 kHz, the maximum single pulse energy was 0.4 mJ, the highest peak power was 325 kW, and the pulse width reached the minimum value of 2.2 ns at 80, 180, 220 and 230 K [88]. In 2019, this team studied the effects of temperature and pump radius on pulsed lasers. The best output performance was achieved when the pulsed laser's temperature was 140 K and the pump light radius was 0.87 mm. The laser's pulse energy was 2.41 mJ, and the corresponding peak power was 1.67 MW [89]. In 2018, Rodenko et al. reported a 343 nm solid-state laser, produced using Yb:YAG/ Cr^{4+} :YAG, to generate a fundamental frequency laser, then frequency doubling is performed by two lithium triborate (LBO) crystals [90]. In 2020, Kim et al. successfully constructed a diode laser pumped passively Q-switched Yb:YAG laser ignitor, which had low power, long pulse width, and a quasi-MW output power [91].

Generally, two temperature controllers are used in passively Q-switched lasers to cool the laser medium and saturable absorber. These increase the volume of the laser and generate additional losses. The volume of the laser and cavity loss can be reduced, and the laser output performance can be improved by using thermal bonding technology to combine the laser medium and saturable absorber into a composite crystal. By direct coating at both ends of the composite crystals, a passive Q-switched microlaser can be formed, which generates pulsed lasers with a high repetition rate and high peak power. The main advantages of the microlaser are its simple structure, low maintenance requirements, and that no fine alignment is required [92–94].

The solid-state waveguide laser is a miniature laser source based on the optical waveguide of the laser material. It has the advantages of small size, high stability, and easy integration, in addition to the waveguide structure being able to effectively reduce the thermal effect on the laser. The combination of Yb^{3+} -doped waveguide laser and Cr^{4+} :YAG can effectively improve the thermal effect of the laser and increase the peak power of the output laser [69,70,95,96].

In 2017, Ye et al. reported a passively Q-switched frequency-switched laser based on a Yb:YAG/Cr⁴⁺:YAG/YAG composite crystal, which achieved simultaneous dual-wavelength laser oscillation at 515 and 524.5 nm. The experimental setup is illustrated in Figure 8 [97].

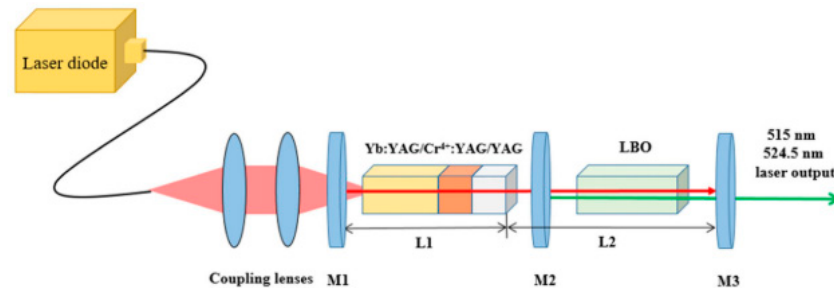


Figure 8. Experimental setup of passive Q-switched frequency-doubled laser based on Yb:YAG/Cr⁴⁺:YAG/YAG composite crystal.

In 2018, Wang et al. demonstrated a multi-wavelength, sub-nanosecond Yb:YAG/Cr⁴⁺:YAG/YVO₄ passively Q-switched Raman microchip laser emitting at 1–1.26 μm . The experimental setup is demonstrated in Figure 9. By adjusting the pump power, the frequency interval can be varied [98].

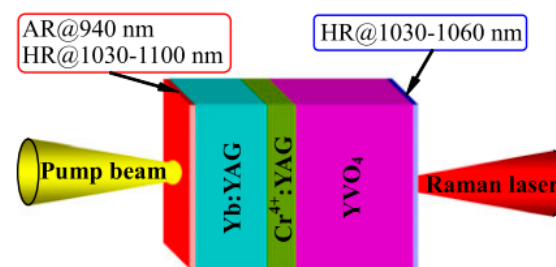


Figure 9. Experimental setup of passive Q-switched Raman laser based on composite crystal Yb:YAG/Cr⁴⁺:YAG/YVO₄.

As crystal growth technology has developed, studies have addressed the specific wavelength requirements of various fields while also improving laser performance. For example, yttrium-doped calcium borate compounds are an excellent active media for passively Q-switched lasers, which can be operated at room temperature [99]. The thermal conductivity of Lu₂O₃ ceramics is 12.5 W/mK (at 300 K), and the thermal conductivity of Lu₂O₃ ceramics will not change significantly even if laser ions with higher concentrations are added [100].

In 2016, Liu et al. reported a Yb:LuPO₄/Cr⁴⁺:YAG passively Q-switched laser that achieved 1013.3 nm pulsed laser output at room temperature. Its pulse repetition rate, pulse energy, duration, and peak power are 23.8 kHz, 22.3 mJ, 4.0 ns, and 5.6 kW, respectively [101]. In 2017, Schoepp et al. reported a Yb:CaF₂/Cr⁴⁺:YAG passively Q-switched laser that achieved a 1050 nm pulsed laser output. The M^2 of the output laser was 1.1, and the peak power, pulse energy, and pulse width were 8.9 kW, 0.7 mJ, and 78 ns, respectively [102]. Subsequently, the same team also reported a compact Yb:YAB passively Q-switched laser using a *c*-cut Yb:YAB crystal and with a laser output of 1041 nm [103]. In 2018, Liu et al. reported the first passive Q-switched laser based on a Yb:GSGG crystal. Its repetition rate, pulse duration, and single pulse energy are 20 kHz, 21 ns, and 38 μJ , respectively [104]. In 2019, David S.P. et al. reported a Yb:Y₂O₃/Cr⁴⁺:YAG ceramic passively Q-switched laser with a single pulse energy of 0.46 mJ, peak power of 1.64 kW, and repetition rate of 19.6 kHz [105]. Additionally, Li et al. reported a Yb:LaCa₄O(BO₃)₃/Cr⁴⁺:YAG passively Q-switched laser with an output light repetition rate of 71 kHz and average power of 3.8 W [106].

2.3. Brief Summary

As the Cr⁴⁺:YAG crystal has a wide transmission range (0.9–1.2 μm) and a particularly strong absorption peak in the 1 μm band, it is frequently used as the passive Q-switch material for Nd³⁺-doped and Yb³⁺-doped lasers. Table 1 lists the research progress on Nd³⁺ and Yb³⁺ passively Q-switched lasers over the last five years. The table summarizes information about the doped ion, laser crystal, center wavelength, peak power, repetition rate, and pulse width.

Table 1. Research progress on Nd³⁺ and Yb³⁺ passively Q-switched lasers in the past five years.

Doped Ion	Time	Experimental Conditions			Output Characteristic	Refs.
		Laser Crystal	Center Wavelength	Cr ⁴⁺ :YAG T ₀		
Nd ³⁺	2016	Nd:YAG	1112 nm	95%	P = 11.2 kW, f = 9 kHz, FWHM = 27.2 ns	[107]
	2016	Nd:YAG	-	20%	P = 5.7 MW, f = 20 Hz, FWHM = 10 ns	[108]
	2017	Nd:YAG	1.06 μm	-	P = 4.55 MW, FWHM = 552 ps	[109] *
	2018	Nd:YAG	1064.48 nm 1064.52 nm	85%	P = 126.4 W, f = 5.8 kHz, FWHM = 42 ns P = 133.6 W, f = 5.8 kHz, FWHM = 40 ns	[110]
	2019	Nd:YAG	1.05 μm	87% 89% 94% 97%	P = 1.9 kW, FWHM = 24 ns P = 1.1 kW, FWHM = 34 ns P = 0.35 kW, FWHM = 51 ns P = 0.09 kW, FWHM = 88 ns	[111]
	2019	Nd:GdTaO ₄	1066 nm	80%	P = 2.34 kW, f = 33.7 kHz, FWHM = 15.2 ns	[112]
	2020	Nd:YAG	1074.1 nm	89.5%	P = 1.6 kW, f = 21.7 kHz, FWHM = 23.7 ns	[113]
	2016	Yb:Lu(WO ₄) ₂	1031 nm	78% 83%	P = 80.3 kW, f = -, FWHM = 0.66 ns P = 69 kW, f = 12.4 kHz, FWHM = 0.69 ns	[114]
Yb ³⁺	2017	Yb:LuPO ₄	1005 nm	85.4%	P = 50.3 kW, f = 19.2 kHz, FWHM = 3.0 ns	[115]
	2017	Yb:KLu(WO ₄) ₂	-	85% 90% 95%	P = 480 W, f = 19 kHz, FWHM = 231 ns P = 190 W, f = 36.2 kHz, FWHM = 347 ns P = 110 W, f = 55.7 kHz, FWHM = 456 ns	[116]
	2018	Yb:LuVO ₄	1.02 μm	99.3%	P = 209 W, f = 285.7 kHz, FWHM = 39.2 ns	[117]
	2018	Yb:KLu(WO ₄) ₂	1030 nm	99.3%	P = 48.5 W, f = 970 kHz, FWHM = 39 ns	[118]
	2019	Yb:YAG	-	85%	P = 67.5–90 kW, f = 1–20 kHz, FWHM = 3–4 ns	[119]
	2020	Yb:YAG	1030 nm	76%	P = 750 kW, f = 8.5 kHz, FWHM = 1.6 ns	[120]

Notes. T₀: the initial transmittances of Cr⁴⁺:YAG; P: peak power; f: repetition rate; FWHM: pulse width; “-” means no relevant data; “*” means the output parameters are measured after the amplifier.

When compared with the Nd³⁺-doped lasers, the main advantage of the Yb³⁺-doped lasers is that the pump and emission wavelengths are close, ensuring a low thermal effect. However, because the emission cross-section of Yb³⁺ ions is much smaller than that of Nd³⁺ ions, a higher pump intensity is required to achieve the given gain.

3. Summary and Outlook

Using Q-switched lasers with Cr⁴⁺:YAG crystal as the saturable absorber can provide high peak power, large pulse energy, high beam quality, and sub-nanosecond pulse width. They have the potential to be widely used in various fields, including high-precision laser processing, space exploration, laser medical treatment, and material analysis. Over the last five years, some unstable features of these lasers have been progressively analyzed and improved upon. In addition, researchers have successfully realized passively Q-switched pulsed laser output of Pr³⁺-doped lasers [121,122] and ceramic lasers [123,124]. Usually, to reduce the lasing threshold, the saturable absorber is placed near the beam waist of

the resonator for higher power density to reach the saturated absorption. In addition, the saturable absorber is usually cooled by thermoelectric cooler (TEC) or water for long-term stable operation, especially in the case of high-power pumping.

In conclusion, an all-solid-state passively Q-switched laser can produce peak power output in the order of megahertz, and its pulse width can be compressed to the order of sub-nanoseconds. Their overall design is becoming more compact and stable. However, all-solid-state passively Q-switched lasers also have limitations, for example, the damage threshold of coating on both ends of crystals is much smaller than that of the laser medium, limiting the peak power and single pulse energy output. With the continuous progress in scientific research and technology, the demand for the output performance of passively Q-switched lasers will continue to increase. Future technical demands will require continued development of all-solid-state passively Q-switched laser performance through research into new doped ions, suitable laser matrices with high doping concentrations, and laser ceramics. Advances in these areas could rapidly lead to the development of lasers with higher energy, narrower pulse width, and better stability.

Author Contributions: Conceptualization, Z.B. and Z.L.; investigation, J.T., and D.Z.; writing—original draft preparation, J.T., D.Z. and Z.B.; writing—review and editing, Z.B., Y.Q. and J.D.; supervision, Z.B., and Z.L.; funding acquisition, Z.B., Y.W. and Z.L. All authors have read and agreed to the published version of the manuscript.

Funding: This work was supported by the National Natural Science Foundation of China (61927815, 61905061 and 62075056), Natural Science Foundation of Hebei Province (F2019202337, and F2019202467), Hebei Science and Technology Innovation Strategy Funding Project (20180601), and Hebei Foundation for Returned Overseas Scholars (C20190177).

Institutional Review Board Statement: No applicable.

Informed Consent Statement: No applicable.

Data Availability Statement: No new data were created or analyzed in this study. Data sharing is not applicable to this article.

Conflicts of Interest: The authors declare no conflict of interest.

References

1. Ma, J.; Dong, J. Advances in Passively Q-Switched Yb³⁺-Doped Laser Materials Microchip Solid-State Lasers. *Chin. J. Lasers* **2010**, *37*, 2278–2288.
2. Li, M.L.; Meng, P.B.; Yan, F.J.; Shi, W.Z.; Feng, W.; Luo, P.P. Research progress of high repetition frequency passively Q-switched solid-state lasers. *LOP* **2015**, *52*, 7–16.
3. Yang, C.W.; Chen, Q.S.; Xiong, K.; Yin, X.D.; Huo, Y.J. Recent Developments on Cr⁴⁺: YAG Passively Q-switched Lasers. *Laser Infrared* **2003**, *1*, 21–24.
4. Kellner, T.; Heine, F.; Huber, G.; Kück, S. Passive Q Switching of a Diode-Pumped 946-nm Nd: YAG Laser with 1.6-W Average Output Power. *Appl. Opt.* **1998**, *37*, 30. [[CrossRef](#)] [[PubMed](#)]
5. Andrauskas, D.M.; Kennedy, C. Tetravalent Chromium Solid-State Passive Q Switch for Nd: YAG Laser Systems. In Proceedings of the Advanced Solid State Lasers, Hilton Head, SC, USA, 18–20 March 1991.
6. Zayhowski, J.J.; Dill, C. Diode-pumped passively Q-switched picosecond microchip lasers. *Opt. Lett.* **1994**, *19*, 1427–1429. [[CrossRef](#)]
7. Mallard, J.; Guillot, D. Up to 350 microJoules with a microchip laser at 1064 nm. In Proceedings of the Conference on Lasers and Electro-Optics Europe, Nice, France, 10–15 September 2000.
8. Pavel, N.; Saikawa, J.; Kurimura, S.; Shoji, I.; Taira, T. Intra-cavity frequency doubling of a Nd: YAG laser passively Q-switched by Cr⁴⁺: YAG saturable absorber. In Proceedings of the Conference on Lasers and Electro-Optics, Baltimore, MD, USA, 11 May 2001.
9. Forget, S.; Druon, F.; Balembois, F.; Georges, P.; Landru, N.; Fève, J.P.; Lin, J.L.; Weng, Z.M. Passively Q-switched diode-pumped Cr⁴⁺: YAG/Nd³⁺: GdVO₄ monolithic microchip laser. *Opt. Commun.* **2006**, *259*, 816–819. [[CrossRef](#)]
10. Tsunekane, M.; Taira, T. High peak power, passively Q-switched Yb: YAG/Cr: YAG micro-lasers. *IEEE J. Quantum Electron.* **2013**, *49*, 454–461. [[CrossRef](#)]
11. Bezotosnyi, V.V.; Gorbunkov, M.V.; Koromyslov, A.L.; Pevtsov, V.F.; Popov, Y.M.; Tunkin, V.G.; Cheshev, E.A. Dual-wavelength generation at the transverse mode locking in a diode-end-pumped passively Q-switched Nd: YLF/Cr⁴⁺: YAG laser. *Bull. Lebedev Phys. Inst.* **2017**, *44*, 1–4. [[CrossRef](#)]

12. Brandus, C.A.; Greculeasa, M.; Broasca, A.; Voicu, F.; Gheorghe, L.; Pavel, N. Diode-pumped bifunctional Nd: LGSB laser passively Q-switched by a Cr⁴⁺: YAG saturable absorber. *Opt. Mater. Express* **2021**, *11*, 685–694. [[CrossRef](#)]
13. Wang, X.L.; Wang, X.J.; Dong, J. Sub-nanosecond, high peak power Yb: YAG/Cr⁴⁺: YAG/YVO₄ passively Q-switched Raman micro-laser operating at 1134 nm. *J. Lumin.* **2021**, *234*, 117955. [[CrossRef](#)]
14. Tsai, S.Y.; Chiu, C.P.; Chang, K.C.; Wei, M.D. Periodic and chaotic dynamics in a passively Q-switched Nd: GdVO₄ laser with azimuthal polarization. *Opt. Lett.* **2016**, *41*, 1054–1057. [[CrossRef](#)]
15. Srivastava, D.K.; Agarwal, A.K. Comparative experimental evaluation of performance, combustion and emissions of laser ignition with conventional spark plug in a compressed natural gas fuelled single cylinder engine. *Fuel* **2014**, *123*, 113–122. [[CrossRef](#)]
16. Agarwal, A.K.; Singh, A.P.; Pal, A. Effect of laser parameters and compression ratio on particulate emissions from a laser ignited hydrogen engine. *Int. J. Hydrogen Energy* **2017**, *42*, 10622–10635. [[CrossRef](#)]
17. Dascalu, T.; Croitoru, G.; Grigore, O.; Pavel, N. High-peak-power passively Q-switched Nd: YAG/Cr⁴⁺: YAG composite laser with multiple-beam output. *Photonics Res.* **2016**, *4*, 267–271. [[CrossRef](#)]
18. Pavel, N.; Tsunekane, M.; Kanehara, K.; Taira, T. Composite all-ceramics, passively Q-switched Nd: YAG/Cr⁴⁺: YAG monolithic micro-laser with two-beam output for multi-point ignition. In Proceedings of the Laser Science to Photonic Applications, Baltimore, MD, USA, 1–6 May 2011.
19. Ma, Y.F.; He, Y.; Yu, X.; Li, X.D.; Li, J.; Yan, R.P.; Peng, J.B.; Zhang, X.L.; Sun, R.; Pan, Y.B.; et al. Multiple-beam, pulse-burst, passively Q-switched ceramic Nd: YAG laser under micro-lens array pumping. *Opt. Express* **2015**, *23*, 24955–24961. [[CrossRef](#)]
20. Lim, H.H.; Taira, T. High peak power Nd: YAG/Cr: YAG ceramic microchip laser with unstable resonator. *Opt. Express* **2019**, *27*, 31307–31315. [[CrossRef](#)] [[PubMed](#)]
21. Tsunekane, M.; Inohara, T.; Ando, A.; Kido, N.; Kanehara, K.; Taira, T. High Peak Power, Passively Q-switched Microlaser for Ignition of Engines. *IEEE J. Quantum Electron.* **2010**, *46*, 277–284. [[CrossRef](#)]
22. Patane, P.; Nandgaonkar, M. Review: Multipoint laser ignition system and its applications to IC engines. *Opt. Laser Technol.* **2020**, *130*, 106305. [[CrossRef](#)]
23. Dong, J.; Bai, S.C.; Liu, S.H.; Ueda, K.I.; Kaminskii, A.A. A high repetition rate passively Q-switched microchip laser for controllable transverse laser modes. *J. Opt.* **2016**, *18*, 055205. [[CrossRef](#)]
24. He, H.S.; Zhang, M.M.; Dong, J.; Ueda, K.I. Linearly polarized pumped passively Q-switched Nd: YVO₄ microchip laser for Ince–Gaussian laser modes with controllable orientations. *J. Opt.* **2016**, *18*, 125202. [[CrossRef](#)]
25. Dong, J.; He, Y.; Bai, S.C.; Ueda, K.I.; Kaminskii, A.A. A Cr⁴⁺: YAG passively Q-switched Nd: YVO₄ microchip laser for controllable high-order Hermite–Gaussian modes. *Laser Phys.* **2016**, *26*, 095004. [[CrossRef](#)]
26. Zhang, M.M.; Bai, S.C.; Dong, J. Effects of Cr⁴⁺ ions on forming Ince–Gaussian modes in passively Q-switched microchip solid-state lasers. *Laser Phys. Lett.* **2019**, *16*, 025003. [[CrossRef](#)]
27. Ma, Y.F.; Peng, Z.F.; Peng, F.; Ding, S.J.; He, Y.; Yu, X.; Zhang, Q.L.; Li, L.J. A diode-pumped Cr⁴⁺: YAG passively Q-switched Nd: GdTaO₄ laser. *Opt. Laser Technol.* **2018**, *108*, 202–206. [[CrossRef](#)]
28. Lan, J.L.; Huang, X.X.; Guan, X.F.; Xu, B.; Xu, H.Y.; Cai, Z.P.; Xu, X.D.; Li, D.Z.; Xu, J. Laser characteristics of Nd³⁺-doped calcium barium niobate ferroelectric crystal at 1.06 and 1.34 μm. *Appl. Opt.* **2017**, *56*, 4191–4196. [[CrossRef](#)] [[PubMed](#)]
29. Xu, X.D.; Di, J.Q.; Zhang, J.; Tang, D.Y.; Xu, J. CW and passively Q-switched laser performance of Nd: Lu₂SiO₅ crystal. *Opt. Mater.* **2016**, *51*, 241–244. [[CrossRef](#)]
30. Cui, Q.; Zhou, Z.Y.; Guan, X.F.; Xu, B.; Lin, Z.; Xu, H.Y.; Cai, Z.P.; Xu, X.D.; Li, D.Z.; Xu, J. Diode-pumped continuous-wave and passively Q-switched Nd: LuAG crystal lasers at 1.1 μm. *Opt. Laser Technol.* **2017**, *96*, 190–195. [[CrossRef](#)]
31. Liang, H.C.; Li, D.; Lin, E.H.; Hsu, C.C.; Lin, H.Y. Investigation of the antiphase dynamics of the orthogonally polarized passively Q-switched Nd: YLF laser. *Opt. Express* **2018**, *26*, 26590–26597. [[CrossRef](#)]
32. Lin, H.Y.; Liu, H.; Chen, Q.; Huang, X.H.; Sun, D. Passively Q-switched Nd: GSGG laser at 936.3 nm. *Optik* **2020**, *211*, 164642. [[CrossRef](#)]
33. Zhang, Y.Y.; Li, J.R.; Hu, Y.Y.; Zhang, H.D.; Qiu, C.C.; Zhang, C.; Wang, X.P.; Liu, B.; Yang, Y.G.; Lv, X.S. Temperature tunable lasers with disordered Nd:ABC₃O₇ crystals. *Opt. Laser Technol.* **2020**, *125*, 106018. [[CrossRef](#)]
34. Ma, Y.F.; Peng, Z.F.; He, Y.; Yao, W.M.; Yan, R.P.; Li, X.D.; Yu, X.; Peng, F.; Zhang, Q.L.; Dou, R.Q. Continuous-wave and passively Q-switched Nd: GYTO₄ laser. *Laser Phys. Lett.* **2017**, *14*, 095802. [[CrossRef](#)]
35. Ma, Y.F.; Sun, H.Y.; Peng, Z.F.; Ding, S.J.; Peng, F.; Yu, X.; Zhang, Q.L. Diode-pumped continuous-wave and passively Q-switched Nd: GdLaNbO₄ laser. *Opt. Mater. Express* **2018**, *8*, 983–991. [[CrossRef](#)]
36. Zong, M.Y.; Zhang, Z.M.; Feng, X.Y.; Zhao, M.F.; Liu, J.; Xu, X.D. Efficient continuous-wave and passively Q-switched lasers based on disordered Nd: Ca_{0.7}La_{0.3}Al₁₂O₁₉ crystals. *Opt. Laser Technol.* **2020**, *125*, 106022. [[CrossRef](#)]
37. Li, Y.B.; Feng, C.; Jia, Z.T.; Zhang, J.; Tao, X.T. Crystal growth, spectra and passively Q-switched laser at 1106 nm of Nd: Gd₃AlGa₄O₁₂ crystal. *J. Alloy Compd.* **2020**, *814*, 152248. [[CrossRef](#)]
38. Lu, H.D.; Mangaiyarkarasi, D. Thermal focal length determination of a laser crystal by modulating the pump source. *Laser Phys.* **2020**, *30*, 066205. [[CrossRef](#)]
39. Naegele, M.; Stoppel, K.; Ridderbusch, H.; Dekorsy, T. Passively Q-switched Nd: YVO₄ laser operating at 914 nm. In Proceedings of the SPIE LASE, San Francisco, CA, USA, 21 February 2020.
40. Li, C.Y.; Dong, J. Pump beam waist-dependent pulse energy generation in Nd: YAG/Cr⁴⁺: YAG passively Q-switched microchip laser. *J. Mod. Opt.* **2016**, *63*, 1323–1330. [[CrossRef](#)]

41. Xing, E.B.; Rong, J.M.; Khew, S.Y.; Tong, C.Z.; Hong, M.H. Thermal lens effect for optimizing a passively Q-switched 1064 nm laser. *Appl. Phys. Express* **2018**, *11*, 062702. [[CrossRef](#)]
42. Koromyslov, A.L.; Tupitsyn, I.M.; Cheshev, E.A. Experimental study of cavity length influence on lasing characteristics Q-Switched Nd: YLF laser. *JPCS* **2020**, *1439*, 012022.
43. Zhang, B.C.; Chen, Y.; Wang, P.Y.; Wang, Y.C.; Liu, J.B.; Hu, S.; Xia, X.S.; Sang, Y.B.; Yuan, H.; Cai, X.L. Direct bleaching of a Cr⁴⁺: YAG saturable absorber in a passively Q-switched Nd: YAG laser. *Appl. Opt.* **2018**, *57*, 4595–4600. [[CrossRef](#)]
44. Fan, Y.M.; Zah, C.E.; Wu, D.H.; Gao, C.; Li, Y.; Liu, X.S. Diode pumped passively Q-switched Nd: YAG/Cr: YAG solid-state lasers with a stable output of millijoules at 1064 nm over a wide temperature range. In Proceedings of the SPIE LASE, San Francisco, CA, USA, 21 February 2020.
45. Song, J.; Li, C.; Ueda, K.I. Thermal influence of saturable absorber in passively Q-switched diode-pumped cw Nd: YAG/Cr⁴⁺: YAG laser. *Opt. Commun.* **2000**, *177*, 307–316. [[CrossRef](#)]
46. Yin, S.M.; Wu, Y.; Sun, N.C. Influence of temperature on Cr⁴⁺: YAG passively Q-switched laser plateau region. *Opt. Optoelect. Technol.* **2010**, *8*, 31–34.
47. Ma, Y.F.; Li, H.J.; Lin, J.P.; Yu, X. A thermally-insensitive passively Q-switched Cr⁴⁺: YAG/Nd: YAG laser. *Opt. Laser Technol.* **2011**, *43*, 1491–1494. [[CrossRef](#)]
48. Nie, M.M.; Liu, Q.; Ji, E.C.; Gong, M.L. End-pumped temperature-dependent passively Q-switched lasers. *Appl. Opt.* **2015**, *54*, 8383–8387. [[CrossRef](#)]
49. Xue, J.W.; Shi, J.Q.; Chen, W.; Pan, Y.; Su, B.H. Temperature dependence of a Cr⁴⁺: YAG passively Q-switched single-longitudinal-mode Nd: YVO₄ ring cavity laser. *Optik* **2017**, *130*, 769–776. [[CrossRef](#)]
50. Zheng, L.H.; Kausas, A.; Taira, T. > MW peak power at 266 nm, low jitter kHz repetition rate from intense pumped microlaser. *Opt. Express* **2016**, *24*, 28748–28760. [[CrossRef](#)]
51. Chen, S.Y.; Yang, H.L.; Wang, M.J.; Zhang, X.; Jiang, J.; Meng, J.Q.; Chen, W.B. Analysis of Natural Longitudinal Mode Selection in Passively Q-Switched Lasers. *Chin. J. Lasers* **2016**, *43*, 0801006. [[CrossRef](#)]
52. Croitoru, G.; Grigore, O.V.; Dinca, M.; Pavel, N.; Bärwinkel, M.; Heinz, P.; Brüggemann, D. Aspects of Air-Breakdown with a High-Peak Power Passively Q-Switched Nd: YAG/Cr⁴⁺: YAG Laser. In Proceedings of the Laser Ignition Conference, Bucharest, Romania, 20–23 June 2017.
53. Villafana, R.E.; Chiu, R.; Mora, G.M.; Casillas, R.F.; Medel, R.C.; Sevilla, E.R. Dynamics of a Q-switched Nd: YVO₄/Cr: YAG laser under periodic modulation. *Results Phys.* **2019**, *12*, 908–913. [[CrossRef](#)]
54. Bai, J.R.; Liu, Y.; Zhong, Z.Y.; Meng, J.; Shi, J.J.; Wang, M.J.; Meng, J.Q.; Hou, X.; Chen, W.B. Narrow Pulse Width lasers Operating over Wide Range of Low Temperature. *Chin. J. Lasers* **2019**, *46*, 0101004.
55. Li, X.D.; Zhou, Y.P.; Yan, R.P.; Wang, D.Y.; Fa, X.; Ma, Y.F.; Zhou, Z.X. A compact pulse burst laser with YAG/Nd: YAG/Cr⁴⁺: YAG composite crystal. *Optik* **2017**, *136*, 107–111. [[CrossRef](#)]
56. Yan, R.P.; Li, X.D.; Zhang, Y.B.; Liu, Z.X.; Wen, X.L.; Chen, D.Y.; Zhou, Z.X. High-repetition-rate, high-peak-power burst mode laser with YAG/Nd: YAG/Cr⁴⁺: YAG composite crystal. *Optik* **2018**, *175*, 263–267. [[CrossRef](#)]
57. Huang, X.S.; Hui, Y.L.; Jiang, M.H.; Lei, H.; Li, Q. Passively Q-switched Nd: YAG/Cr⁴⁺: YAG micro laser with high beam quality. In Proceedings of the International Symposium on Optoelectronic Technology and Application 2016, Beijing, China, 9–11 May 2016.
58. Xue, J.W.; Pan, Y.; Chen, W.; Fang, Y.J.; Xie, H.J.; Xie, M.Y.; Sun, L.; Su, B.H. Cr: YAG passively Q-switched single-frequency Nd: YVO₄ ring cavity laser. *JOSA B* **2016**, *33*, 1815–1819.
59. Xue, F.; Zhang, S.S.; Cong, Z.H.; Huang, Q.J.; Guan, C.; Wu, Q.W.; Chen, H.; Bai, F.; Liu, Z.J. Diode-end-pumped single-longitudinal-mode passively Q-switched Nd: GGG laser. *Laser Phys. Lett.* **2018**, *15*, 035001. [[CrossRef](#)]
60. Negri, J.R.; Pirzio, F.; Agnesi, A. Passively Q-switched single-frequency Nd: YVO₄ ring laser with external feedback. *Opt. Express* **2018**, *26*, 11903–11908. [[CrossRef](#)] [[PubMed](#)]
61. Negri, J.R.; Pirzio, F.; Agnesi, A. Jitter investigation of narrow-bandwidth passively Q-switched Nd: YAG unidirectional ring laser. *Opt. Lett.* **2019**, *44*, 3094–3097. [[CrossRef](#)] [[PubMed](#)]
62. Chen, T.; Chen, X.; Zhou, C.L.; Li, M.; Shu, R. Single-longitudinal-mode-operated, passively Q-switched Nd: YAG/Cr⁴⁺: YAG microchip laser with 100 kHz repetition rate and 400 ps pulse width. *Appl. Opt.* **2020**, *59*, 4191–4197. [[CrossRef](#)] [[PubMed](#)]
63. Wang, J.X.; Zhang, W.Z.; Wang, Q.Y.; Xing, Q.R.; Deng, P.Z.; Xu, J.; Qiao, Z.W. Passive Mode-Locking in a CPM Nd: YAG Laser Using Cr⁴⁺: YAG. *Acta Opt. Sin.* **1998**, *18*, 24–28.
64. Chen, Y.F.; Tsai, S.; Wang, S.C. High-power diode-pumped Q-switched and mode-locked Nd: YVO₄ laser with a Cr⁴⁺: YAG saturable absorber. *Opt. Lett.* **2000**, *25*, 1442–1444. [[CrossRef](#)]
65. Zhang, S.J.; Wu, E.; Zeng, H.P. Q-switched mode-locking by Cr⁴⁺: YAG in a laser-diode-pumped c-cut Nd: GdVO₄ laser. *Opt. Commun.* **2004**, *231*, 365–369. [[CrossRef](#)]
66. Ng, S.P.; Tang, D.Y.; Kong, J.; Qin, L.J.; Meng, X.L.; Xiong, Z.J. Q-switched and continuous-wave mode-locking of a diode-pumped Nd: Gd_{0.64}Y_{0.36}VO₄–Cr⁴⁺: YAG laser. *Appl. Phys. B* **2005**, *81*, 511–515. [[CrossRef](#)]
67. Tian, W.; Wang, C.; Wang, G.; Liu, S.; Liu, J. Performance of diode-pumped passively Q-switched mode-locking Nd: GdVO₄/KTP green laser with Cr⁴⁺: YAG. *Laser Phys. Lett.* **2006**, *4*, 196. [[CrossRef](#)]
68. Liu, F.Q.; He, J.L.; Xu, J.L.; Zhang, B.T.; Yang, J.F.; Xu, J.Q.; Gao, C.Y.; Zhang, H.J. Passively Q-switched mode-locking in a diode-pumped c-cut Nd: LuVO₄ laser with Cr⁴⁺: YAG. *Laser Phys. Lett.* **2009**, *6*, 567. [[CrossRef](#)]

69. Jelínek, M. Functional planar thin film optical waveguide lasers. *Laser Phys. Lett.* **2011**, *9*, 91–99. [[CrossRef](#)]
70. Beach, R.J.; Mitchell, S.C.; Meissner, H.E.; Meissner, O.R.; Krupke, W.F.; McMahon, J.M.; Bennett, W.J.; Shepherd, D.P. Continuous-wave and passively Q-switched cladding-pumped planar waveguide lasers. *Opt. Lett.* **2001**, *26*, 881–883. [[CrossRef](#)] [[PubMed](#)]
71. Mackenzie, J.I. Dielectric solid-state planar waveguide lasers: A review. *IEEE J. Sel. Top. Quantum Electron.* **2007**, *13*, 626–637. [[CrossRef](#)]
72. Zhou, H.Q.; Zhu, S.Q.; Jiang, W.; Li, Z.; Wang, Y.C.; Yin, H.; Chen, Z.Q.; Yuan, J. Diode-end-pumped passively Q-switched blue laser with Nd: YAG/YAG/Cr⁴⁺: YAG/YAG composite crystal. *Optik* **2016**, *127*, 10588–10592. [[CrossRef](#)]
73. Zhang, X.Z.; Zhou, Y.; Yasukevich, A.; Loiko, P.; Mateos, X.; Xu, X.G.; Guo, S.Y.; Wang, Z.P. Diode-pumped passively Q-switched self-frequency-doubled Nd: CNGS laser. *Opt. Express* **2017**, *25*, 19760–19766. [[CrossRef](#)]
74. Zhou, Y.; Wang, Z.P.; Chen, F.F.; Yu, F.P.; Xu, X.G. 1 kW Peak Power Self-Frequency-Doubling Microchip Laser. *IEEE Photonics J.* **2019**, *11*, 1–5. [[CrossRef](#)]
75. Wang, X.J.; Wang, X.L.; Zheng, Z.F.; Qiao, X.H.; Dong, J. 1164.4 nm and 1174.7 nm dual-wavelength Nd: GdVO₄/Cr⁴⁺: YAG/YVO₄ passively Q-switched Raman microchip laser. *Appl. Opt.* **2018**, *57*, 3198–3204. [[CrossRef](#)]
76. Duan, Y.M.; Zhang, J.; Zhu, H.Y.; Zhang, Y.C.; Xu, C.W.; Wang, H.Y.; Fan, D.Y. Compact passively Q-switched RbTiOPO₄ cascaded Raman operation. *Opt. Lett.* **2018**, *43*, 4550–4553. [[CrossRef](#)] [[PubMed](#)]
77. Jiang, C.; Chen, Y.Y.; Mei, S.H.; Zhu, S.Q.; Li, Z.; Jiang, W.; Zhou, H.Q.; Chen, Z.Q.; Ji, E.C. Investigation of a passively Q-switched Raman laser at 1176 nm with Nd³⁺: YAG/Cr⁴⁺: YAG/YAG composite crystal and a coupled cavity. *Opt. Quantum Electron.* **2019**, *51*, 380. [[CrossRef](#)]
78. Lin, H.Y.; Pan, X.; Huang, X.H.; Xiao, M.; Liu, X.; Sun, D.; Zhu, W.Z. Multi-wavelength passively Q-switched c-cut Nd: YVO₄ self-Raman laser with Cr⁴⁺: YAG saturable absorber. *Opt. Commun.* **2016**, *368*, 39–42. [[CrossRef](#)]
79. Lin, H.Y.; Pan, X.; Huang, X.H.; Xiao, M.; Liu, X.; Sun, D.; Zhu, W.Z. Cr⁴⁺: YAG passively Q-switched c-cut Nd: YVO₄ self-Raman laser at 1168.6 nm. *Infrared Phys. Technol.* **2016**, *75*, 56–58. [[CrossRef](#)]
80. Chen, M.T.; Dai, S.B.; Zhu, S.Q.; Yin, H.; Li, Z.; Chen, Z.Q. Multi-watt passively Q-switched self-Raman laser based on a c-cut Nd: YVO₄ composite crystal. *J. Opt. Soc. Am. B* **2019**, *36*, 524–532. [[CrossRef](#)]
81. Li, S.T.; Jin, G.Y.; Dong, Y. Simultaneous three Raman shift passively Q-switched intracavity Raman laser based on the overlapping Raman shift of 259 cm⁻¹ in c-cut GdVO₄ and YVO₄. *Appl. Phys. B* **2020**, *126*, 37. [[CrossRef](#)]
82. Chen, Y.F.; Chang, C.C.; Lee, C.Y.; Sung, C.L.; Tung, J.C.; Su, K.W.; Liang, H.C.; Chen, W.D.; Zhang, G. High-peak-power large-angular-momentum beams generated from passively Q-switched geometric modes with astigmatic transformation. *Photonics Res.* **2017**, *5*, 561–566. [[CrossRef](#)]
83. Tuan, P.H.; Liang, H.C.; Huang, K.F.; Chen, Y.F. Realizing high-pulse-energy large-angular-momentum beams by astigmatic transformation of geometric modes in an Nd: YAG/Cr⁴⁺: YAG laser. *IEEE J. Sel. Top. Quantum Electron.* **2018**, *24*, 1–9. [[CrossRef](#)]
84. Pan, Y.; Zhang, M.M.; Dong, J. Orientation and separation controllable dual-vortex passively Q-switched microchip laser. *J. Opt.* **2019**, *21*, 085202. [[CrossRef](#)]
85. Fan, T.Y. Heat generation in Nd: YAG and Yb: YAG. *IEEE J. Quantum Electron.* **1993**, *29*, 1457–1459. [[CrossRef](#)]
86. Ertel, K.; Banerjee, S.; Mason, P.D.; Phillips, P.J.; Siebold, M.; Hernandez, G.C.; Collier, J.C. Optimising the efficiency of pulsed diode pumped Yb: YAG laser amplifiers for ns pulse generation. *Opt. Express* **2011**, *19*, 26610–26626. [[CrossRef](#)] [[PubMed](#)]
87. Li, Q.Q.; Chen, X.Z.; Fan, S.G. Study on the preparation and properties of Yb: YAG glass ceramics. *J. Synth. Cryst.* **2010**, *39*, 163–168.
88. Šulc, J.; Eisenschreiber, J.; Jelínková, H.; Nejezchleb, K.; Škoda, V. Influence of temperature on Yb: YAG/Cr: YAG microchip laser operation. In Proceedings of the SPIE LASE, San Francisco, CA, USA, 17 February 2017.
89. Šulc, J.; Eisenschreiber, J.; Němec, M.; Jelínková, H.; Nejezchleb, K.; Škoda, V. Temperature and Pumping Beam Radius Influence on Yb: YAG/Cr: YAG Microchip Laser Output. In Proceedings of the CLEO/Europe-EQEC, Munich, Germany, 23–27 June 2019.
90. Rodenko, O.; Tidemand, L.P.; Pedersen, C. Low repetition rate 343 nm passively Q-switched solid-state laser for time-resolved fluorescence spectroscopy. *Opt. Express* **2018**, *26*, 20614–20621. [[CrossRef](#)]
91. Kim, J.; Moon, S.; Park, Y.; Kim, H.S. Optimization of a Passively Q-switched Yb: YAG Laser Ignitor Pumped by a Laser Diode with Low Power and Long Pulse Width. *Curr. Opt. Photonics* **2020**, *4*, 127–133.
92. Guo, X.Y.; Tokita, S.; Kawanaka, J. 12 mJ Yb: YAG/Cr: YAG microchip laser. *Opt. Lett.* **2018**, *43*, 459–461. [[CrossRef](#)] [[PubMed](#)]
93. Li, J.Z.; Chen, Z.Q.; Zhu, S.Q. High-peak-power and short-pulse laser with a Yb: YAG/Cr⁴⁺: YAG/YAG composite crystal. *Infrared Laser Eng.* **2018**, *47*, 606007-0606007.
94. Li, J.Z.; Zhu, S.Q. High-peak-power short-pulse laser using a Yb: YAG/Cr⁴⁺: YAG/YAG composite crystal. *Optik* **2019**, *176*, 630–635. [[CrossRef](#)]
95. Mackenzie, J.I.; Shepherd, D.P. End-pumped, passively Q-switched Yb: YAG double-clad waveguide laser. *Opt. Lett.* **2002**, *27*, 2161–2163. [[CrossRef](#)] [[PubMed](#)]
96. Lei, H.; Liu, Q.; Wang, Y.; Hui, Y.L.; Zhu, Z.D.; Li, Q. Passively Q-switched pulse laser with large core size crystal waveguide near diffraction-limit beam quality output. *Acta Opt. Sin.* **2021**, *41*, 1214001.
97. Ye, P.P.; Zhu, S.Q.; Li, Z.; Yin, H.; Zhang, P.X.; Fu, S.H.; Chen, Z.Q. Passively Q-switched dual-wavelength green laser with an Yb: YAG/Cr⁴⁺: YAG/YAG composite crystal. *Opt. Express* **2017**, *25*, 5179–5185. [[CrossRef](#)] [[PubMed](#)]
98. Wang, X.L.; Wang, X.J.; Dong, J. Multi-wavelength, Sub-Nanosecond Yb: YAG/Cr⁴⁺: YAG/YVO₄ Passively Q-Switched Raman Microchip Laser. *IEEE J. Sel. Top. Quantum Electron.* **2018**, *24*, 1–8.

99. Mougél, F.; Dardenne, K.; Aka, G.; Kahn-Harari, A.; Vivien, D. Ytterbium-doped $\text{Ca}_4\text{GdO}(\text{BO}_3)_3$: An efficient infrared laser and self-frequency doubling crystal. *J. Opt. Soc. Am. B* **1999**, *16*, 164–172. [[CrossRef](#)]
100. David, S.P.; Jambunathan, V.; Yue, F.X.; Le Garrec, B.J.; Lucianetti, A.; Mocek, T. Laser performances of diode pumped Yb: Lu_2O_3 transparent ceramic at cryogenic temperatures. *Opt. Mater. Express* **2019**, *9*, 4669–4676. [[CrossRef](#)]
101. Liu, J.H.; Wang, L.S.; Han, W.J.; Xu, H.H.; Zhong, D.G.; Teng, B. Plate-shaped Yb: LuPO_4 crystal for efficient CW and passively Q-switched microchip lasers. *Opt. Mater.* **2016**, *60*, 114–118. [[CrossRef](#)]
102. Schoepp, T.R.; Tiedje, H.F.; Fedosejevs, R. Characterisation and Modelling of a Passively Q-Switched Yb: CaF_2 Laser. *IEEE J. Quantum Electron.* **2017**, *53*, 1–8. [[CrossRef](#)]
103. Serres, J.M.; Loiko, P.A.; Mateos, X.; Liu, J.H.; Zhang, H.J.; Yumashev, K.; Griebner, U.; Petrov, V.; Aguiló, M.; Díaz, F. Multi-watt passively Q-switched Yb: YAB/Cr: YAG microchip lasers. In Proceedings of the SPIE LASE, San Francisco, CA, USA, 17 February 2017.
104. Liu, Q.Y.; Yuan, H.L.; Dai, X.J.; Zhang, Y.; Zhao, Y.G.; Xu, H.H.; Pan, Z.B. Efficient pulsed laser operation of Yb-doped $\text{Gd}_3\text{Sc}_2\text{Ga}_3\text{O}_{12}$ mixed crystal. *Opt. Eng.* **2018**, *57*, 096103. [[CrossRef](#)]
105. David, S.P.; Jambunathan, V.; Yue, F.X.; Lucianetti, A.; Mocek, T. Efficient diode pumped Yb: Y_2O_3 cryogenic laser. *Appl. Phys. B* **2019**, *125*, 137. [[CrossRef](#)]
106. Li, Y.H.; Xu, Y.F.; Dong, L.; Han, W.J.; Xu, H.H.; Liu, J.H. Passively Q-switched laser action of Yb: $\text{LaCa}_4\text{O}(\text{BO}_3)_3$ crystal. *Laser Phys.* **2019**, *29*, 085801. [[CrossRef](#)]
107. Dun, Y.Y.; Li, P.; Chen, X.H.; Ma, B.M. High-power passively Q-switched Nd: YAG laser at 1112 nm with a Cr^{4+} : YAG saturable absorber. *Chin. Phys. Lett.* **2016**, *33*, 024201.
108. Maleki, A.; Saghafifar, H.; Tehrani, M.K.; Soltanolkotabi, M.; Baghi, M.D.; Ardestani, M.M. 57ám] with 10áns passively Q-switched diode pumped Nd: YAG laser using Cr^{4+} : YAG crystal. *Opt. Quantum Electron.* **2016**, *48*, 48. [[CrossRef](#)]
109. Lee, H.C.; Chang, D.W.; Lee, E.J.; Yoon, H.W. High-energy, sub-nanosecond linearly polarized passively Q-switched MOPA laser system. *Opt. Laser Technol.* **2017**, *95*, 81–85. [[CrossRef](#)]
110. Zhou, Y.; Jiao, M.X.; Lian, T.H.; Xing, J.H.; Liu, Y.; Liu, J.N. Design and Experimental Investigation of Passively Q-Switched Two-Cavity Dual-Frequency Nd: YAG Laser. *Chin. J. Lasers* **2018**, *45*, 1201008. [[CrossRef](#)]
111. Koromyslov, A.L.; Tupitsyn, I.M.; Cheshev, E.A. Dual-wavelength Q-switched laser based on a lens-shaped Nd: YAG active element and a Cr^{4+} : YAG passive Q-switch. *Quantum Electron.* **2019**, *49*, 95. [[CrossRef](#)]
112. Liu, Y.; Yan, R.P.; Wu, W.T.; Li, X.D.; Dong, Z.; Liu, Z.X.; Wen, X.L.; Yao, W.M.; Peng, F.; Zhang, Q.L. High-repetition-rate passively Q-switched Nd: GdTaO_4 1066 nm laser under 879 nm pumping. *Infrared Phys. Technol.* **2019**, *102*, 103025. [[CrossRef](#)]
113. Lin, H.Y.; Huang, X.H.; Liu, H. Passively Q-switched Nd: YAG laser at 1074.1 nm. *Optik* **2020**, *207*, 163831. [[CrossRef](#)]
114. Loiko, P.; Serres, J.M.; Mateos, X.; Yumashev, K.; Yasukevich, A.; Petrov, V.; Griebner, U.; Aguiló, M.; Díaz, F. Sub-nanosecond Yb: $\text{KLu}(\text{WO}_4)_2$ microchip laser. *Opt. Lett.* **2016**, *41*, 2620–2623. [[CrossRef](#)]
115. Wang, L.S.; Han, W.J.; Xu, H.H.; Zhong, D.G.; Teng, B.; Liu, J.H. Passively Q-switched oscillation at 1005–1012 nm of a miniature Yb: LuPO_4 crystal rod laser. *Laser Phys. Lett.* **2017**, *14*, 045807. [[CrossRef](#)]
116. Navratil, P.; Jambunathan, V.; David, S.P.; Yue, F.X.; Serres, J.M.; Mateos, X.; Aguiló, M.; Díaz, F.; Griebner, U.; Petrov, V. Continuous-wave and passively Q-switched cryogenic Yb: $\text{KLu}(\text{WO}_4)_2$ laser. *Opt. Express* **2017**, *25*, 25886–25893. [[CrossRef](#)] [[PubMed](#)]
117. Dou, X.D.; Yang, J.N.; Ma, Y.J.; Han, W.J.; Xu, H.H.; Liu, J.H. Passive Q-switching of a Yb: LuVO_4 laser with Cr^{4+} : YAG: Approaching the intrinsic upper limit of repetition rate. *Chin. Phys. Lett.* **2018**, *35*, 064201. [[CrossRef](#)]
118. Tian, K.; Dou, X.D.; Yi, H.Y.; Han, W.J.; Xu, H.H.; Liu, J.H. Anomalous passive Q-switching induced by Cr^{4+} : YAG: With pulse repetition rate approaching up to 1 MHz. *Laser Phys.* **2018**, *29*, 015805. [[CrossRef](#)]
119. Bourdon, P.; Planchat, C.; Fleury, D.; Le, G.J.; Gustave, F.; Dolfi, B.A.; Lombard, L.; Durecu, A.; Jacqmin, H. Passively cooled Cr: YAG Q-switched Yb: YAG micro-laser delivering continuously tunable high repetition rate bursts of short pulses. In Proceedings of the SPIE LASE, San Francisco, CA, USA, 7 March 2019.
120. McIntosh, C.; Hays, A.; Chinn, S.; Goldberg, L.; Leach, J. High average power passively Q-switched Yb: YAG micro-laser. In Proceedings of the SPIE LASE, San Francisco, CA, USA, 21 February 2020.
121. Tanaka, H.; Kariyama, R.; Iijima, K.; Hirose, K.; Kannari, F. Saturation of 640-nm absorption in Cr^{4+} : YAG for an InGaN laser diode pumped passively Q-switched Pr^{3+} : YLF laser. *Opt. Express* **2015**, *23*, 19382–19395. [[CrossRef](#)]
122. Tanaka, H.; Kariyama, R.; Iijima, K.; Kannari, F. 50-kHz, 50-ns UV pulse generation by diode-pumped frequency doubling Pr^{3+} : YLF Q-switch laser with a Cr^{4+} : YAG saturable absorber. *Appl. Opt.* **2016**, *55*, 6193–6198. [[CrossRef](#)]
123. He, Y.; Ma, Y.F.; Li, J.; Li, X.D.; Yan, R.P.; Gao, J.; Yu, X.; Sun, R.; Pan, Y.B. Continuous-wave and passively Q-switched 1.06 μm ceramic Nd: YAG laser. *Opt. Laser Technol.* **2016**, *81*, 46–49. [[CrossRef](#)]
124. Ma, Y.F.; He, Y.; Peng, Z.F.; Yan, R.P.; Li, X.D.; Yu, X.; Tong, Y.; Ge, L.; Li, J.; Tittel, F.K. Doubly Q-switched tape casting YAG/Nd: YAG/YAG ceramic laser. *J. Mod. Opt.* **2018**, *65*, 1549–1553. [[CrossRef](#)]